Carbohydrate Polymers 90 (2012) 1197–1203

Contents lists available at SciVerse ScienceDirect

Carbohydrate Polymers

journal homepage: www.elsevier.com/locate/carbpol

Exploring the conformational space of amorphous cellulose using NMR chemical shifts

Tetsuya Mori[a,b], Eisuke Chikayama[c,d], Yuuri Tsuboi[e], Nobuhiro Ishida[a], Noriko Shisa[f], Yoshiyuki Noritake[f], Shigeharu Moriya[d,e,g], Jun Kikuchi[b,c,d,g,*]

[a] Biotechnology Laboratory, Toyota Central R&D Laboratories, Inc., 41-1, Nagakute 480-1192, Japan
[b] Graduate School of Bioagricultural Sciences, Nagoya University, 1 Furo-cho, Chikusa-ku, Nagoya 464-0810, Japan
[c] RIKEN Plant Science Center, 1-7-22 Suehiro-cho, Tsurumi-ku, Yokohama 230-0045, Japan
[d] Graduate School of Nanobiosciences, Yokohama City University, 1-7-29 Suehiro-cho, Tsurumi-ku, Yokohama 230-0045, Japan
[e] RIKEN Advanced Science Institute, 2-1 Hirosawa, Wako 351-0198, Japan
[f] Organic Material Engineering Division, Toyota Motor Corp., 1 Toyota-cho, Toyota 471-8572, Japan
[g] Biomass Engineering Program, RIKEN Research Cluster for Innovation, 2-1 Hirosawa, Wako 351-0198, Japan

ARTICLE INFO

Article history:
Received 3 February 2012
Received in revised form 6 June 2012
Accepted 11 June 2012
Available online 19 June 2012

Keywords:
Amorphous cellulose
Ionic liquid
2D NMR
Computer simulation

ABSTRACT

^{13}C-labeled amorphous cellulose and ^{13}C NMR chemical shifts by 2D ^{13}C–^{13}C correlation spectroscopy were obtained in the regenerated solid-state from ionic liquids. On the basis of the assigned chemical shifts, combined with information from molecular dynamics and quantum chemistry computer simulations a twisted structure for amorphous cellulose is proposed exposing more hydrophilic surface than that of extended crystalline cellulose.

1. Introduction

Cellulose is the most common chemical polymer on land. It is used in diverse materials such as fibers produced from cotton, paper generated from wood, food, cosmetics, biomedical materials, separation membranes, films, and various other industrial materials (Berlioz, Molina-Boisseau, Nishiyama, & Heux, 2009; Galbe & Zacchi, 2007; Klemm, Heublein, Fink, & Bohn, 2005; Mai, Kues, & Militz, 2004; Rubin, 2008; Somerville, Youngs, Taylor, Davis, & Long, 2010). Advances in genomic science have indicated new plants useful for industrial production of biomass including trees (Kubo et al., 2005; Zhong, Demura, & Ye, 2006), and biomass engineering technology is being developed to use this biomass (Jarboe et al., 2010). In the future, the majority of synthetic polymers from fossil resources are expected to be replaced by cellulose products (Demirbas, 2009).

Cellulose is composed of crystalline and amorphous structures (Hesse-Ertelt, Witter, Ulrich, Kondo, & Heinze, 2008). Many researchers have elucidated its crystal structures in detail using X-ray or NMR observations. Their works suggest that these structures can be classified as cellulose I and cellulose II, which are believed to contain molecular chains in parallel (Hieta, Kuga, & Usuda, 1984; Kuga & Brown, 1988) and antiparallel (Langan, Nishiyama, & Chanzy, 1999) alignment, respectively. Amorphous cellulose is disordered and thus its structural properties are largely unknown (Dadi, Varanasi, & Schall, 2006; Wickholm, Larsson, & Iversen, 1998; Zhao et al., 2009). However, there have been several studies of it's physical properties (Dadi et al., 2006; Zhao et al., 2009).

Amorphous cellulose can be obtained experimentally from regenerated cellulose, although regenerated cellulose typically takes the form of cellophane, or common cloth fibers such as rayon, cuprammonium, or lyocell, which are extracted from pulp. The regeneration process involves sequential dissolution of cellulose in a solvent, and then removal of the solvent to fix the molecular conformation. Although cellulose has traditionally been mercerized by the application of alkali (Heines, 1944) and its solubility is increased by acetylation (Pravotorova, Baibakova, & Maiboroda, 1973), these

* Corresponding author at: RIKEN Plant Science Center, 1-7-22 Suehiro-cho, Tsurumi-ku, Yokohama 230-0045, Japan. Tel.: +81 45 503 9490; fax: +81 45 503 9489.
E-mail addresses: tmori@psc.riken.jp (T. Mori), chika@psc.riken.jp (E. Chikayama), tsuboyu@psc.riken.jp (Y. Tsuboi), e1168@mosk.tytlabs.co.jp (N. Ishida), noriko@shisa.tec.toyota.co.jp (N. Shisa), noritake@giga.tec.toyota.co.jp (Y. Noritake), smoriya@riken.jp (S. Moriya), kikuchi@psc.riken.jp (J. Kikuchi).

0144-8617/$ – see front matter.
http://dx.doi.org/10.1016/j.carbpol.2012.06.027

methods require the use of toxic solvents that adversely affect the environment. Ionic liquids, which are environmentally benign solutions consisting of cations and anions, are expected to be good candidates as new solubilizing agents for cellulose (Swatloski, Spear, Holbrey, & Rogers, 2002). Several researchers have found that the rate of cellulose dissolution differs according to the type of ionic liquid used (Fukaya, Hayashi, Wada, & Ohno, 2008; Pinkert, Marsh, Pang, & Staiger, 2009; Remsing, Swatloski, Rogers, & Moyna, 2006; Swatloski et al., 2002; Zhang, Zhang, Wu, He, & Xiang, 2010).

The atomic structure of crystalline cellulose was first elucidated by XRD (Meyer & Mark, 1928). Because solid-state NMR spectroscopy showed natural crystalline cellulose consisted of two types, it has been used as a structural analysis tool (Atalla & Vanderhart, 1984). A ^{13}C labeling technique has been used to analyze ^{13}C–^{13}C or ^{13}C–^{1}H spin coupling transfer in atomic groups for each type of cellulose structure, and the types were assigned according to a conformation-dependent chemical shift observed for cellulose samples (Kono, Erata, & Takai, 2003; Kono, Numata, Erata, & Takai, 2004; Masuda et al., 2003). Solid-state NMR spectroscopy also enabled observation of the amorphous structure of cellulose (Wickholm et al., 1998). However, not all carbon atoms were assigned, because C2, C3, and C5 overlap in 1D ^{13}C NMR spectra.

Although many molecular dynamics simulations of crystalline cellulose have been published (French, Miller, & Aabloo, 1993; Miyamoto et al., 2009), only a few researchers have simulated amorphous cellulose (Queyroy, Neyertz, Brown, & Muller-Plathe, 2004). The features of amorphous cellulose cannot be elucidated by XRD. Compared with crystalline cellulose, the amorphous counterpart probably contains fewer hydrogen bonds and increased flexibility (Shen, Langan, French, Johnson, & Gnanakaran, 2009).

Liu et al. analyzed structural changes in cellulose pretreated with an ionic liquid by examining the distribution of torsion angles associated with the glycosidic linkage using a molecular dynamics simulation (Liu, Sale, Holmes, Simmons, & Singh, 2010). Because the change in torsion angles reflects the chemical shift, conformational changes in cellulose can be monitored using NMR spectroscopy. More detailed analyses have been performed using quantum chemistry calculations (Suzuki, Horii, & Kurosu, 2009). The crystal structure of cellulose Iα has been refined using its chemical shift and molecular dynamics simulations (Witter et al., 2006), and the 3D structure of oligosaccharides has been studied using their chemical shift and *ab initio* chemical shift simulations (Sergeyev & Moyna, 2005). A *de novo* structural model can be constructed by combining the results of chemical shift analyses and simulations. Although an amorphous cellulose model has been developed by combining the results of chemical shift analyses and simulations, the model was not characterized by comparison with crystal structure data (Sergeyev & Moyna, 2005).

Using solid-state NMR spectroscopy, we fully assigned the NMR spectrum of regenerated amorphous ^{13}C-labeled cellulose. Based on the chemical shifts of the cellulose structure, we also proposed a local structure for amorphous cellulose that was determined on computer using experimental NMR chemical shifts. ^{13}C labeling of cellulose enabled solid state 2D NMR spectra to be obtained; the resulting improved separation of ^{13}C–^{13}C spin-coupling-based cross peaks allowed complete assignment of the chemical shifts for the C1–C6 positions. This technique allowed the overlap of the C2, C3, and C5 signals of amorphous cellulose to be resolved for the first time. The content of amorphous structure in cellulose regenerated in several ionic liquids allowed the amorphous state for which we made the assignments to be validated. Importantly, we clarified the atomic structure of amorphous cellulose for the first time. Because we developed a method in which experimental chemical shifts are coupled with an ensemble of computer-simulated molecular conformations, we were able to determine a quasi-stable local structure of amorphous cellulose, which was compared with crystal structure data for crystalline cellulose.

2. Experimental

2.1. Chemicals

$^{13}C_6$-glucose (98% ^{13}C) and DMSO-d_6 (99.9% D) were purchased from Cambridge Isotope Laboratories (Andover, MA). $^{13}C_2$-sodium acetate was purchased from Shoko (Tokyo, Japan). The ionic liquids 1-ethyl-3-methylimidazolium diethylphosphate ([Emim][DEP]), 1-ethyl-3-methylimidazolium chloride ([Emim][Cl]), and 1-ethyl-3-methylimidazolium acetate ([Emim][Ac]) were obtained from Kanto Chemical (Tokyo, Japan). Purelox for washing cellulose pellicles was obtained from Oyalox (Tokyo, Japan).

2.2. Preparation of NMR samples

2.2.1. ^{13}C Uniform stable isotope labeling of bacterial cellulose

Acetobacter xylinum (NBRC 15237) was cultured in sterilized Hestrin–Schramm medium (Hestrin & Schramm, 1954) containing $^{13}C_6$-glucose. This culture medium was incubated statically at 30 °C for 14 days. After cultivation, the cellulose pellicles were washed sequentially with 10% Purelox, 4% NaOH, isopropanol, and distilled water to remove metabolites, proteins, cell walls and membranes, respectively. The cellulose pellicles were dried at 65 °C for 12 h.

2.2.2. Solid-state NMR samples

^{13}C-cellulose (10 mg) was added to an ionic liquid (1.0 g) and incubated at 120 °C for 30 min. After incubation in one of three different ionic liquids, the cellulose samples were regenerated by adding distilled water (5 g), stirring, and washing by filtration (filter unit, Nalgene, Rochester, NY). The cellulose was dried under reduced pressure at 60 °C for 4 h.

2.3. NMR analysis

Solid powder cellulose samples were inserted into a ZrO_2 rotor with a diameter of 4 mm. All solid-state NMR spectra were recorded on a DRX-800 spectrometer (Bruker Biospin, Billerica, MA) operating at 800.200 MHz for ^{1}H and 200.050 MHz for ^{13}C with a 4 mm Magic-Angle Spinning (MAS) triple resonance probe maintained at 298 K using a Bruker X-tream temperature control unit. 1D ^{13}C cross-polarization (CP) MAS and 2D ^{13}C–^{13}C refocused incredible natural abundance double quantum transfer experiment (INADEQUATE) NMR spectra (Lesage, Bardet, & Emsley, 1999) were taken at 12 kHz MAS and a CP contact time of 1 ms. A total of 256 complex f1 and 2048 complex f2 points were recorded using 64 scans per f1 increment. The spectral widths and offset frequencies were 161,290 Hz (120 ppm) and 80,645 Hz (120 ppm) for f1 and f2, respectively, the recycle delay was set to 4.0 s, and the τ delay was set to 2.0 ms for refocused INADEQUATE analysis. ^{13}C chemical shifts were calibrated using the methyl carbon resonance of ^{13}C-sodium acetate as an internal reference at 26.8 ppm, which corresponds to tetramethylsilane at 0 ppm. NMR spectra were processed using NMRPipe software (Delaglio et al., 1995).

2.4. Computer simulated analysis of 5000 generated structures

The nuclear coordinates of a cellobiose molecule in a vacuum were generated manually using a procedure identical to that employed to determine the coordinates of cellulose Iα (Nishiyama, Sugiyama, Chanzy, & Langan, 2003). From the initial coordinates of cellobiose, five simulations of the molecular dynamics at 298 K in a vacuum were calculated using GROMACS software (http://www.gromacs.org/). These simulations

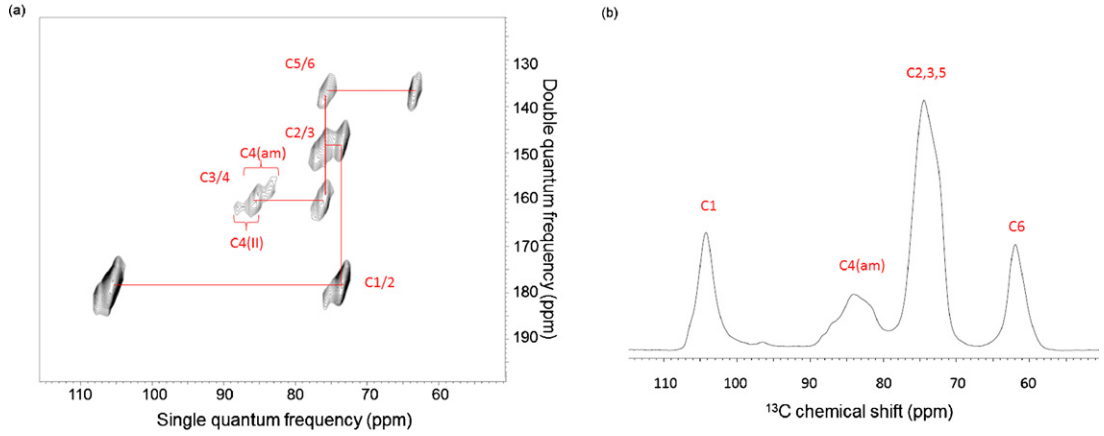

Fig. 1. (a) Solid-state ^{13}C–^{13}C refocused INADEQUATE spectrum of cellulose pretreated with [Emim][Cl]. Solid lines indicate connections between neighboring carbons and represent the amorphous cellulose signal. A small amount of cellulose II was detected at a chemical shift of 88.2 ppm in the C3/4 region. (b) Solid-state ^{13}C NMR spectra of cellulose pretreated with [Emim][Cl].

ran for 20 ps each with a time step of 2 fs. One thousand structures were generated per simulation, giving a total of 5000 cellobiose structures. The isotropic shielding constants for these structures were calculated with the program Gaussian 09 (http://www.gaussian.com/g_prod/g09.htm) using the Restricted Hartree-Fock theoretical level and the 6–31G(d) basis set to approximate the wave function of the system (Ditchfie, Hehre, & Pople, 1971; Frisch, Pople, & Binkley, 1984; Hehre, Ditchfie, & Pople, 1972; Hehre, Stewart, & Pople, 1969). The shielding constants were calibrated with experimental chemical shifts to generate computational chemical shifts. From the computational chemical shifts, we further determined the relative differences between the calculated chemical shifts of C1–C4 and those for cellulose Iα. The torsion angles ϕ and φ for O5-C1-O1-C4′ and C1-O1-C4′-C3′, respectively, were determined. The centers of three regions in the molecule were determined from local maxima of ϕ in the density distribution. These three regions are designated CS_1 (*Chemical Shift 1*), CS_2, and CS_3. The top 50 representative structures for the three regions were extracted according to their center and then sorted by their distances. Accessible surface areas were calculated using AREAIMOL (http://www.ccp4.ac.uk/html/areaimol.html). Chimera (http://www.cgl.ucsf.edu/chimera/) was used to display the structures.

2.5. Method of comparison between two chemical shifts

Our newly proposed method is based on the difference in chemical shift between two neighboring atoms in a structure. This method was developed to avoid contributions from remote interactions in chemical shifts, and is applicable to structural elucidation of locally ordered structures even if the global structures are disordered, as in amorphous cellulose. The chemical shift for the C4 atoms in cellobiose can be separated into two terms, $CSC4 = CSC4(neighbor) + CSC4(remote)$, where CSC4 indicates the chemical shift of C4, *neighbor* indicates the contribution to the C4 chemical shift from interactions with neighboring atoms, and *remote* indicates that from remote interactions, because chemical shifts are affected by energy interactions in general. Similarly, $CSC1 = CSC1(neighbor) + CSC1(remote)$ for the chemical shift for C1. Our method can handle experimentally observed chemical shifts such as that derived from the average value of the chemical shifts for a structural ensemble, for example, $\overline{CSC4} = \overline{CSC4(neighbor) + CSC4(remote)} = \overline{CSC4(neighbor)} + \overline{CSC4(remote)}$, where $\overline{CSC4}$ is the experimental chemical shift for C4, or the average value of the structural ensemble. The difference between the experimental chemical shifts for C1 and C4, $\overline{CSC1} - \overline{CSC4} = \overline{CSC1(neighbor) + CSC1(remote) - CSC4(neighbor) - CSC4(remote)}$, becomes $\overline{CSC1(neighbor) - CSC4(neighbor)} = \overline{CSC1(neighbor)} - \overline{CSC4(neighbor)}$ when the remote terms cancel each other out, *i.e.*, $\overline{CSC1(remote)} = \overline{CSC4(remote)}$. We can predict that $\overline{CSC1(remote)} = \overline{CSC4(remote)}$ because C4 and C1 are in structural proximity along the glycosidic bond, and thus the difference in chemical shift between the C4 and C1 atoms caused by remote interactions is believed to be small. Therefore, $\overline{CSC1} - \overline{CSC4}$ can be simplified to $\overline{CSC1(neighbor)} - \overline{CSC4(neighbor)}$, or *the average chemical shift for C1 relative to that for C4 reflecting only the local structural conformation about C1 and C4*. The theoretical chemical shifts for each generated structure were compared on the basis of $\overline{CSC1} - \overline{CSC4} = \sum_{i=1}^{N}\{CSC1(i) - CSC4(i)\}/N$, where $CSC1(i)$ and $CSC4(i)$ are the theoretical chemical shifts for C1 and C4, respectively, in the ith structure of the structural ensemble (N).

3. Results and discussion

3.1. Complete 2D NMR assignment of ^{13}C-labeled amorphous cellulose

Full assignment of 2D NMR spectra of solid-state ^{13}C-labeled amorphous cellulose (Fig. 1, Table 1) consisting of bacterial ^{13}C-cellulose obtained from *A. xylinum* was achieved. To do this, we used 2D ^{13}C–^{13}C refocused INADEQUATE spectroscopy to determine the NMR assignments for ^{13}C-labeled solid-state amorphous cellulose. Cross correlations appeared clearly in the 2D INADEQUATE spectrum (Fig. 1a) with an increased signal-to-noise ratio because of ^{13}C-labeling. In a 2D INADEQUATE spectrum, the *y* axis corresponds to pairs of adjacent atoms where each cross peak is the sum of the chemical shifts for each of these atoms, so the values on the *y* axis are approximately doubled. Starting at the known C1 chemical shifts, we could determine the C1/2 cross peak and the C1 and C2 chemical shifts in the 2D spectrum of solid-state amorphous cellulose. The C1/2 cross peak indicates that there is a chemical bond between C1 and C2. This allowed the two cross peaks at 75.1 (*x* axis) and 146.8 (*y* axis) ppm, and 75.4 (*x* axis) and 148.1 (*y* axis) ppm to be identified as C2/3 cross peaks (Fig. 1a), but two candidates resided above and below the C2/3 peak for the next assignment. This ambiguity was resolved by the C6 chemical shift deduced from an additional solution state experiment with an ionic liquid (data not shown). This revealed that the cross peak above the C2/3 peak (at 136.9 ppm on the *y* axis, Fig. 1a) and the uppermost right-hand cross peak were those for the C6 and C5 chemical shifts,

Table 1
Assignment of peaks in solid-state ^{13}C NMR spectra of cellulose (ppm). In cellulose regenerated from [Emim][Cl], chemical shifts in parentheses were obtained from 1D CP-MAS data.

Sample	C1	C2	C3	C4	C5	C6	Experiment
Untreated	105.3			89.2 84.0		65.6 62.5	1D CP-MAS
Regenerated from [Emim][Cl]	105.0	72.8	75.1	85.0	74.8	62.7 (62.7)	Refocused INADEQUATE (1D CP-MAS)
	104.8 (105.0)	72.6	75.4	84.5 83.1 82.8 (84.8)			

respectively. The chemical shift for C6 was 62.7 ppm (Fig. 1a). The split peaks at 85.0, 84.5, 83.1, and 82.8 ppm on the *x* axis and 160.8, 159.6, 158.5, and 158.0 ppm on the *y* axis were assigned to the chemical shifts of C4 in a mixture of crystalline and amorphous states. The assignment of C4 is consistent with the relative positions of the peaks in a solution-state experiment (data not shown) and made more sense than the alternative possibility, which was assigning these peaks to C6. Therefore, we fixed the assignments of C4 and C6, which also allowed us to fix the C3/4 and C4/3 cross peaks. Finally, the C4/5 and C5/4 cross peaks could be determined using the same overlapping positions of C3/4 and C4/3 that were required to link the C5/4 and C5/6 cross peaks. Consequently, the C3 chemical shifts were identified as those 75.1 and 75.4 ppm, and the C5 chemical shift was as attributed to the signal at 74.8 ppm. The chemical shift assignments for 1D ^{13}C CP-MAS were also completed (Fig. 1b). A small amount of cellulose II was found in the 2D refocused INADEQUATE spectrum for the regenerated cellulose (Fig. 1a), although the signals from amorphous cellulose dominated. The C4 chemical shifts exhibited the largest differences for the carbon atoms in the cellulose structures (Isogai, Usuda, Kato, Uryu, & Atalla, 1989). Therefore, the C4 chemical shifts can be used to distinguish cellulose I, cellulose II, and amorphous cellulose (Kono et al., 2003, 2004; Wickholm et al., 1998).

The complete NMR assignments of amorphous cellulose (Table 1) offer the basis of the expected elucidation of the structure. Assignment of the C2 and C3 chemical shifts has additional value for studying the structural patterns of inter-hydrogen bonding. Hydrogen atoms linked to C2 and C3 are involved in inter-hydrogen bonding (Langan et al., 1999; Nishiyama, Langan, & Chanzy, 2002; Nishiyama et al., 2003), and knowing the interrelation between cellulose chains is important for understanding the degradation process of cellulose (Gao, Chen, Wang, Zhang, & Liu, 2001; Nimlos et al., 2007). Discriminating between C2 and C3 atoms, which had not been achieved before this study, enables analysis of the C2 and C3 intensity or the chemical shifts. A ^{13}C-labeling technique can be adopted for such an experiment. This technique also has advantages for effective multidimensional ^{13}C NMR measurements (Dadi et al., 2006; Kikuchi & Hirayama, 2007; Kikuchi, Shinozaki, & Hirayama, 2004; Lapierre et al., 1983; Okushita, Chikayama, & Kikuchi, 2012). ^{13}C-labeling has the potential for application to biomass polymers, such as cellulose, hemicellulose, pectin, and lignin, (Cadars, Lesage, & Emsley, 2005; Chikayama, Suto, Nishihara, Shinozaki, & Kikuchi, 2008; Dick-Perez et al., 2011; Nakanishi et al., 2011; Sekiyama, Chikayama, & Kikuchi, 2010, 2011; Sekiyama & Kikuchi, 2007; Tian et al., 2007) in studies of cellulose degradation, which would enable discrete ^{13}C–^{13}C correlation NMR experiments in the solid states. Putative assignments of amorphous cellulose for C1, C4, and C6 have been made (Larsson, Westermark, & Iversen, 1995; Larsson, Wickholm, & Iversen, 1997; Wickholm et al., 1998). Our complete assignments will offer a more detailed method of analyzing such experimental NMR systems.

3.2. Assignment of NMR spectra to obtain a representative set of amorphous structures

The C4 chemical shifts for cellulose samples containing different ratios of structural states that were generated in the ionic liquids [Emim][DEP], [Emim][Ac], and [Emim][Cl] were validated to compare amorphous cellulose with other structural states such as cellulose I or II using the C4 chemical shift in the same ionic liquids. Cellulose was completely solubilized in each ionic liquid at 120 °C for 30 min, and then regenerated by addition of water followed by evaporation prior to obtaining solid-state NMR measurements.

The solid-state NMR ^{13}C CP-MAS spectra of cellulose pretreated with different ionic liquids indicated that the cellulose structure regenerated from [Emim][Cl] was the most adequate for structural investigation of the representative structures of amorphous cellulose. From the solid-state NMR spectra, we could distinguish both the C4 chemical shift and relative quantities of the I, II, and amorphous states of cellulose, which could be used to compare the amorphous C4 chemical shift with other structural states (Fig. S1). Untreated bacterial cellulose consisting of cellulose I (C4 chemical shift at 89.2 ppm) and amorphous cellulose (C4 at 84.0 ppm) was used as a control (Fig. S1a). Cellulose pretreated with [Emim][Cl] (Fig. S1b) formed almost entirely amorphous cellulose (C4 at 84.8 ppm), while that treated with [Emim][DEP] (Fig. S1c) formed a mixture of cellulose II (C4 at 87.6 ppm) and amorphous cellulose (C4 at 84.4 and 84.2 ppm). That treated with [Emim][Ac] (Fig. S1d) also formed a mixture of cellulose II (C4 at 87.6 ppm) and amorphous cellulose (C4 at 84.8 and 84.6 ppm). Because [Emim][Cl] produced a larger proportion of amorphous cellulose, this sample was used for 2D NMR experiments so that the assignments made should reveal representative structures of amorphous cellulose. Cellulose samples pretreated with [Emim][Cl] and 1-butyl-3-methylimidazolium chloride ([Bmim][Cl]) have been reported to form amorphous cellulose on the basis of NMR and XRD analysis (Dadi et al., 2006; Zhao et al., 2009).

The differences in the solid-state chemical shifts of C1–C4, which is 0 ppm for cellulose Iα (Witter et al., 2006), were compared to high-resolution (HR) MAS data and values reported in the literature (see Supplementary Experimental). Such comparison allowed a candidate for a local structure of amorphous cellulose to be elucidated (refer to Section 3.3). Values were comparable in the amorphous region above 3.5 ppm, indicating that our results for amorphous cellulose covered a range of amorphous structures. Other atoms were also compared using solid-state NMR spectroscopy (Fig. S2).

3.3. Elucidation of a computer-simulated candidate for a local structure of amorphous cellulose

Three quasi-stable local structures of cellulose were determined *via* computer simulation as a first step toward selecting candidate

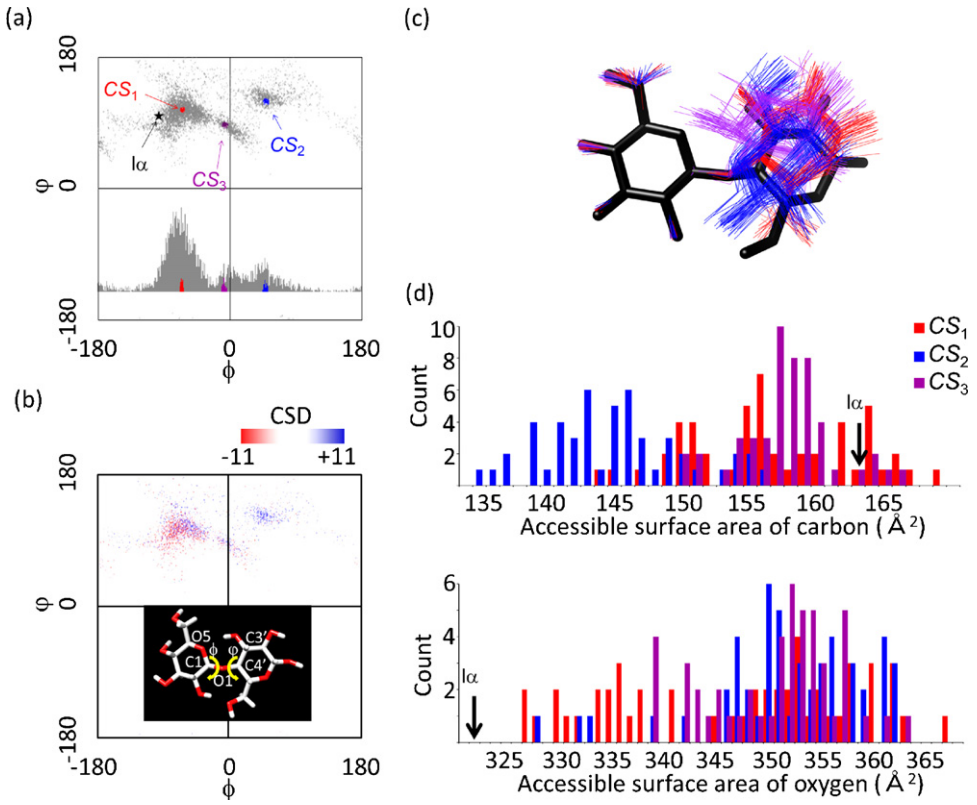

Fig. 2. (a) Distribution of torsion angles (ϕ, φ) of 5000 calculated structures. No structures exist for $\varphi = 0$ to -150°. In this region, the distribution of the torsion angle ϕ is shown. The regions CS_1–CS_3 were energetically quasi-stable states. (b) Distribution of torsion angles (ϕ, φ) of the chemical shifts of 5000 structures. Colors are centered at zero, which is equal to the chemical shift difference of C1–C4 for cellulose Iα, to visualize deviations in the chemical shifts from those of cellulose Iα. CSD: chemical shift difference C1–C4. The structure of a cellobiose molecule is also shown. (c) Superposition of 50 structures for each of CS_1, CS_2, and CS_3. (d) Distribution of the accessible surfaces of carbon (top panel) and oxygen (bottom panel) atoms for 50 structures for each of CS_1–CS_3. (For interpretation of the references to color in this figure legend, the reader is referred to the web version of the article.)

structures of amorphous cellulose (Fig. 2a). Here, 'local structure' means a small part of a large cellulose molecule, *i.e.*, a few atoms and chemical bonds that adopt, on average, a fixed 3D structure. The local structures were represented by a cellobiose molecule in a vacuum, which is a substructure of a cellulose molecule. We used five molecular dynamics simulations of 20 ps to generate 5000 different conformations of a cellobiose molecule. The simulations started from an initial structure of crystallized cellulose I (Nishiyama et al., 2003), which was identical to that obtained by XRD, and then formed disordered states. We identified three dominant regions, CS_1, CS_2, and CS_3, in the dihedral map by analyzing the two torsion angles ϕ and φ along the glycosidic bond for the 5000 structures (Fig. 2a). The region CS_1 was (ϕ, φ) = (-110° to -30°, 60° to 150°), CS_2 was (ϕ, φ) = (20° to 80°, 110° to 150°), and CS_3 was (ϕ, φ) = (-20° to 30°, 50° to 110°). These regions formed energetically quasi-stable states during the simulations. The results obtained for 20 ps simulations are similar to those found for a significantly longer simulation for 10 ns (Fig. S3), so we selected 20 ps as the simulation duration to reduce computation time. In all three regions, φ did not change greatly, while ϕ showed characteristic values. In terms of overall conformations, ϕ changed freely, whereas the φ changed in a limited region between 30° and 180°. This behavior is caused by collisions between moieties in the cellobiose molecule such as C_2—O—H on the ϕ side or C_3—O—H on the φ side. Conflicts between moieties are known to be solved when the system's temperature is high enough (Shen et al., 2009). Our calculations were performed in a vacuum, but the results are consistent with those of Shen et al. (2009) using solvents. They reported a major region corresponding to CS_1 and CS_3, and a region corresponding to CS_2 on their (ϕ, φ) map, although they defined the torsion angles ϕ and φ slightly differently. They also found that an additional region appeared at high temperature. Other studies found that the region corresponding to CS_1 in our study is a global minimum energy state (Mazeau & Heux, 2003; Shen et al., 2009). We selected 50 representative structures in each region (Fig. 2a, red, blue, and purple) for further analyses, as described below.

By comparing the C1 and C4 chemical shifts, we determined that the CS_2 region is representative of a computer-simulated candidate for a local structure of amorphous cellulose based on experimentally determined chemical shifts. The theoretical chemical shifts for C1 and C4, and the difference between C1 and C4 were first determined by quantum chemical calculations for all of the 5000 generated structures. To visualize the contributions of CS_1, CS_2, and CS_3 structures in these chemical shifts, we calculated the relative differences of C1–C4 chemical shifts between those calculated for the theoretical chemical shifts for all of the CS_1, CS_2, and CS_3 structures and those for the crystal structure of cellulose Iα (Fig. 2b) (Witter et al., 2006). This allowed the CS_2 and $CS_1 - CS_3$ regions to be discriminated (Fig. 2b, blue- and red-intensive, respectively). The CS_2 chemical shifts are closer to those of the amorphous structure than those of the crystal structure, while the latter are more similar to that of the crystal structure. Therefore, CS_2 is hypothesized to be representative of an amorphous state. The proposed method can extract average local structures from globally disordered structures, enabling structural investigation of amorphous cellulose.

To evaluate this hypothesis further, the selected representative sets of 50 structures each for CS_1, CS_2, and CS_3 (Fig. 2a, red, blue, and purple, respectively) were examined using statistical tests. The results showed a significant difference in chemical

shifts between CS_2 and either CS_1 (significance probability p (or p value) = 2.55×10^{-6}) or CS_3 ($p = 2.84 \times 10^{-5}$), whereas no significant difference was observed between CS_1 and CS_3 ($p = 0.100$), which confirmed that CS_2 differed from both CS_1 and CS_3 in chemical shift, while CS_1 and CS_3 were similar (Fig. S4). The average chemical shifts of the other carbon atoms, C2, C3, C5, and C6, in CS_1–CS_3 with respect to Iα were also calculated (Fig. S5). The chemical shifts in the CS_2 regions tended to indicate amorphous cellulose, except for that of C6. The reason for this is that C6 was allowed to rotate freely. Problems related to this rotation need further consideration. By combining the test results and our hypothesis, we could conclude that, of the three detected regions, the CS_2 region lies within the most plausible set of quasi-stable local structures of amorphous cellulose. We superimposed the 50 structures each for CS_1, CS_2, and CS_3 (Fig. 2c, red, blue, and purple, respectively). The representative local structures of amorphous cellulose (Fig. 2c, blue) appear on a pyranose ring in a flipped state caused by the increase in ϕ compared to the crystal state. The CS_3 region seems to consist of intermediate structures between those of CS_1 and CS_2.

The candidate local structure of amorphous cellulose possesses a surface that is significantly less hydrophobic than that of crystalline cellulose. We analyzed the solvent-accessible surface for each set of 50 3D coordinates for the CS_1, CS_2, and CS_3 regions (Fig. 2d). The accessible surfaces were classified with respect to those on carbon and oxygen atoms (Fig. 2d, top and bottom, respectively). Consequently, we concluded that the hydrophobic accessible surface (accessible surface on carbon atoms) for CS_2 differed significantly from that for both CS_1 ($p = 7.55 \times 10^{-14}$) and CS_3 ($p = 5.32 \times 10^{-18}$), and was less than those for CS_1, CS_3, and crystalline cellulose I (Fig. 2d). The difference between CS_2 and either CS_1 ($p = 9.70 \times 10^{-3}$) or CS_3 ($p = 6.53 \times 10^{-1}$) was not significant for the accessible surface on oxygen atoms; however, the decreased hydrophobic surface on carbon atoms can be interpreted as amorphous states being preferentially exposed in a hydrophilic solvent to minimize their hydrophobic surface. The average accessible surfaces for carbon atoms for the 50 representative structures were 156.3, 144.5, and 157.0 Å^2 for CS_1, CS_2, and CS_3, respectively. Those for oxygen were 346.4, 351.1, and 350.1 Å^2 for CS_1, CS_2, and CS_3 respectively. The CS_2 region exhibited a decrease of approximately 10% because C2 (φ side), C5 (φ side), and C6 (φ side) were smaller compared to those of CS_1 and CS_3, although a compensatory increase in C1 (ϕ side) affected by the C_6–O moiety was detected. The increased hydrophilicity of the surface in the proposed quasi-stable local amorphous structure, CS_2, should increase its solubility in a polar solvent because of decreased hydrophobic surface area.

4. Conclusion

The atoms in regenerated amorphous cellulose were fully assigned by solid-state 2D ^{13}C–^{13}C NMR spectroscopy, and a candidate local structure of amorphous cellulose was proposed by using both assigned experimental and theoretical chemical shifts. We consider our results are an important step towards detailed elucidation of the structure of amorphous cellulose.

Acknowledgments

The authors thank Haruo Takahashi, Akinori Ikeuchi, and Chie Imamura (Toyota Central R&D Laboratories) for valuable discussion, and Tomohiro Iikura (Yokohama City University) for quantum calculations. This research was supported in part by Grants-in-Aid for Scientific Research for Challenging Exploratory Research (JK), and from the Ministry of Education, Culture, Sports, Science, and Technology, Japan. This work was also partially supported by grants from the New Energy and Industrial Technology Development Organization (NEDO, JK). The authors are grateful for the use of the computational resources of the RIKEN Integrated Cluster of Clusters (RICC) supercomputer system.

Appendix A. Supplementary data

Supplementary data associated with this article can be found, in the online version, at http://dx.doi.org/10.1016/j.carbpol.2012.06.027.

References

Atalla, R. H., & Vanderhart, D. L. (1984). Native cellulose—A composite of 2 distinct crystalline forms. *Science*, *223*(4633), 283–285.
Berlioz, S., Molina-Boisseau, S., Nishiyama, Y., & Heux, L. (2009). Gas-phase surface esterification of cellulose microfibrils and whiskers. *Biomacromolecules*, *10*(8), 2144–2151.
Cadars, S., Lesage, A., & Emsley, L. (2005). Chemical shift correlations in disordered solids. *Journal of the American Chemical Society*, *127*(12), 4466–4476.
Chikayama, E., Suto, M., Nishihara, T., Shinozaki, K., & Kikuchi, J. (2008). Systematic NMR analysis of stable isotope labeled metabolite mixtures in plant and animal systems: Coarse grained views of metabolic pathways. *PLoS ONE*, *3*(11), e3805.
Dadi, A. P., Varanasi, S., & Schall, C. A. (2006). Enhancement of cellulose saccharification kinetics using an ionic liquid pretreatment step. *Biotechnology and Bioengineering*, *95*(5), 904–910.
Delaglio, F., Grzesiek, S., Vuister, G. W., Zhu, G., Pfeifer, J., & Bax, A. (1995). NMRPipe: A multidimensional spectral processing system based on UNIX pipes. *Journal of Biomolecular NMR*, *6*(3), 277–293.
Demirbas, M. F. (2009). Biorefineries for biofuel upgrading: A critical review. *Applied Energy*, *86*, S151–S161.
Dick-Perez, M., Zhang, Y., Hayes, J., Salazar, A., Zabotina, O. A., & Hong, M. (2011). Structure and interactions of plant cell-wall polysaccharides by two- and three-dimensional magic-angle-spinning solid-state NMR. *Biochemistry*, *50*(6), 989–1000.
Ditchfie, R., Hehre, W. J., & Pople, J. (1971). Self-consistent molecular-orbital methods. 9. Extended Gaussian-type basis for molecular-orbital studies of organic molecules. *Journal of Chemical Physics*, *54*(2), 724–728.
French, A. D., Miller, D. P., & Aabloo, A. (1993). Miniature crystal models of cellulose polymorphs and other carbohydrates. *International Journal of Biological Macromolecules*, *15*(1), 30–36.
Frisch, M., Pople, J., & Binkley, J. (1984). Self-consistent molecular-orbital methods. 25. Supplementary functions for Gaussian-basis sets. *Journal of Chemical Physics*, *80*(7), 3265–3269.
Fukaya, Y., Hayashi, K., Wada, M., & Ohno, H. (2008). Cellulose dissolution with polar ionic liquids under mild conditions: Required factors for anions. *Green Chemistry*, *10*(1), 44–46.
Galbe, M., & Zacchi, G. (2007). Pretreatment of lignocellulosic materials for efficient bioethanol production. *Advances in Biochemical Engineering/Biotechnology*, *108*, 41–65.
Gao, P. J., Chen, G. J., Wang, T. H., Zhang, Y. S., & Liu, J. (2001). Non-hydrolytic disruption of crystalline structure of cellulose by cellulose binding domain and linker sequence of cellobiohydrolase I from *Penicillium janthinellum*. *Acta Biochimica et Biophysica Sinica*, *33*(1), 13–18.
Hehre, W., Ditchfie, R., & Pople, J. (1972). Self-consistent molecular-orbital methods. 12. Further extensions of Gaussian-type basis sets for use in molecular-orbital studies of organic-molecules. *Journal of Chemical Physics*, *56*(5), 2257–2261.
Hehre, W., Stewart, R., & Pople, J. (1969). Self-consistent molecular-orbital methods. I. Use of Gaussian EXPANSIONS of Slater-Type atomic orbitals. *Journal of Chemical Physics*, *51*(6), 2657–2664.
Heines, S. V. (1944). John Mercer and mercerization, 1844. *Journal of Chemical Education*, *21*(9), 430.
Hesse-Ertelt, S., Witter, R., Ulrich, A. S., Kondo, T., & Heinze, T. (2008). Spectral assignments and anisotropy data of cellulose I-alpha: C-13-NMR chemical shift data of cellulose I-alpha determined by INADEQUATE and RAI techniques applied to uniformly C-13-labeled bacterial celluloses of different *Gluconacetobacter* xylinus strains. *Magnetic Resonance in Chemistry*, *46*(11), 1030–1036.
Hestrin, S., & Schramm, M. (1954). Synthesis of cellulose by *Acetobacter xylinum*. II. Preparation of freeze-dried cells capable of polymerizing glucose to cellulose. *Biochemical Journal*, *58*(2), 345–352.
Hieta, K., Kuga, S., & Usuda, M. (1984). Electron staining of reducing ends evidences a parallel-chain structure in valonia cellulose. *Biopolymers*, *23*(10), 1807–1810.
Isogai, A., Usuda, M., Kato, T., Uryu, T., & Atalla, R. H. (1989). Solid-state CP MAS C-13 NMR-study of cellulose polymorphs. *Macromolecules*, *22*(7), 3168–3172.
Jarboe, L. R., Zhang, X., Wang, X., Moore, J. C., Shanmugam, K. T., & Ingram, L. O. (2010). Metabolic engineering for production of biorenewable fuels and chemicals: Contributions of synthetic biology. *Journal of Biomedicine and Biotechnology*, *2010*. ID 761042
Kikuchi, J., & Hirayama, T. (2007). Practical aspects of uniform stable isotope labeling of higher plants for heteronuclear NMR-based metabolomics. *Methods in Molecular Biology*, *358*, 273–286.

Kikuchi, J., Shinozaki, K., & Hirayama, T. (2004). Stable isotope labeling of *Arabidopsis thaliana* for an NMR-based metabolomics approach. *Plant and Cell Physiology*, *45*(8), 1099–1104.

Klemm, D., Heublein, B., Fink, H. P., & Bohn, A. (2005). Cellulose: Fascinating biopolymer and sustainable raw material. *Angewandte Chemie-International Edition in English*, *44*(22), 3358–3393.

Kono, H., Erata, T., & Takai, M. (2003). Determination of the through-bond carbon–carbon and carbon–proton connectivities of the native celluloses in the solid state. *Macromolecules*, *36*(14), 5131–5138.

Kono, H., Numata, Y., Erata, T., & Takai, M. (2004). C-13 and H-1 resonance assignment of mercerized cellulose II by two-dimensional MAS NMR spectroscopies. *Macromolecules*, *37*(14), 5310–5316.

Kubo, M., Udagawa, M., Nishikubo, N., Horiguchi, G., Yamaguchi, M., Ito, J., et al. (2005). Transcription switches for protoxylem and metaxylem vessel formation. *Genes & Development*, *19*(16), 1855–1860.

Kuga, S., & Brown, R. M. (1988). Silver labeling of the reducing ends of bacterial cellulose. *Carbohydrate Research*, *180*(2), 345–350.

Langan, P., Nishiyama, Y., & Chanzy, H. (1999). A revised structure and hydrogen-bonding system in cellulose II from a neutron fiber diffraction analysis. *Journal of the American Chemical Society*, *121*(43), 9940–9946.

Lapierre, C., Gaudillere, J. P., Monties, B., Guittet, E., Rolando, C., & Lallemand, J. Y. (1983). Photosynthetic C-13 enrichment of poplar lignins—Preliminary studies by acidolysis and C-13 NMR. *Holzforschung*, *37*(5), 217–224.

Larsson, P. T., Westermark, U., & Iversen, T. (1995). Determination of the cellulose I alpha allomorph content in a tunicate cellulose by CP/MAS C-13-NMR spectroscopy. *Carbohydrate Research*, *278*(2), 339–343.

Larsson, P. T., Wickholm, K., & Iversen, T. (1997). A CP/MAS C-13 NMR investigation of molecular ordering in celluloses. *Carbohydrate Research*, *302*(1–2), 19–25.

Lesage, A., Bardet, M., & Emsley, L. (1999). Through-bond carbon–carbon connectivities in disordered solids by NMR. *Journal of the American Chemical Society*, *121*(47), 10987–10993.

Liu, H., Sale, K. L., Holmes, B. M., Simmons, B. A., & Singh, S. (2010). Understanding the interactions of cellulose with ionic liquids: A molecular dynamics study. *Journal of Physical Chemistry B*, *114*(12), 4293–4301.

Mai, C., Kues, U., & Militz, H. (2004). Biotechnology in the wood industry. *Applied Microbiology and Biotechnology*, *63*(5), 477–494.

Masuda, K., Adachi, M., Hirai, A., Yamamoto, H., Kaji, H., & Horii, F. (2003). Solid-state C-13 and H-1 spin diffusion NMR analyses of the microfibril structure for bacterial cellulose. *Solid State Nuclear Magnetic Resonance*, *23*(4), 198–212.

Mazeau, K., & Heux, L. (2003). Molecular dynamics simulations of bulk native crystalline and amorphous structures of cellulose. *Journal of Physical Chemistry B*, *107*(10), 2394–2403.

Meyer, K. H., & Mark, H. (1928). The structure of the crystallised components of cellulose. *Berichte der Deutschen Chemica Gesellschaft*, *61B*, 593–614.

Miyamoto, H., Umemura, M., Aoyagi, T., Yamane, C., Ueda, K., & Takahashi, K. (2009). Structural reorganization of molecular sheets derived from cellulose II by molecular dynamics simulations. *Carbohydrate Research*, *344*(9), 1085–1094.

Nakanishi, Y., Fukuda, S., Chikayama, E., Kimura, Y., Ohno, H., & Kikuchi, J. (2011). Dynamic omics approach identifies nutrition-mediated microbial interactions. *Journal of Proteome Research*, *10*(2), 824–836.

Nimlos, M. R., Matthews, J. F., Crowley, M. F., Walker, R. C., Chukkapalli, G., Brady, J. V., et al. (2007). Molecular modeling suggests induced fit of Family I carbohydrate-binding modules with a broken-chain cellulose surface. *Protein Engineering Design & Selection*, *20*(4), 179–187.

Nishiyama, Y., Langan, P., & Chanzy, H. (2002). Crystal structure and hydrogen-bonding system in cellulose Ibeta from synchrotron X-ray and neutron fiber diffraction. *Journal of the American Chemical Society*, *124*(31), 9074–9082.

Nishiyama, Y., Sugiyama, J., Chanzy, H., & Langan, P. (2003). Crystal structure and hydrogen bonding system in cellulose I(alpha) from synchrotron X-ray and neutron fiber diffraction. *Journal of the American Chemical Society*, *125*(47), 14300–14306.

Okushita, K., Chikayama, E., & Kikuchi, J. (2012). Solubilization mechanism and characterization of the structural change of bacterial cellulose in regenerated states through ionic liquid treatment. *Biomacromolecules*.

Pinkert, A., Marsh, K. N., Pang, S., & Staiger, M. P. (2009). Ionic liquids and their interaction with cellulose. *Chemical Reviews*, *109*(12), 6712–6728.

Pravotorova, Y. I., Baibakova, N. T., & Maiboroda, Z. V., VI. (1973). Accelerated dissolving of cellulose acetate. *Fibre Chemistry*, *4*(2), 137–139.

Queyroy, S., Neyertz, S., Brown, D., & Muller-Plathe, F. (2004). Preparing relaxed systems of amorphous polymers by multiscale simulation: Application to cellulose. *Macromolecules*, *37*(19), 7338–7350.

Remsing, R. C., Swatloski, R. P., Rogers, R. D., & Moyna, G. (2006). Mechanism of cellulose dissolution in the ionic liquid 1-n-butyl-3-methylimidazolium chloride: a ^{13}C and $^{35/37}Cl$ NMR relaxation study on model systems. *Chemistry Communications (Cambridge)*, *12*, 1271–1273.

Rubin, E. M. (2008). Genomics of cellulosic biofuels. *Nature*, *454*(7206), 841–845.

Sekiyama, Y., Chikayama, E., & Kikuchi, J. (2010). Profiling polar and semipolar plant metabolites throughout extraction processes using a combined solution-state and high-resolution magic angle spinning NMR approach. *Analytical Chemistry*, *82*(5), 1643–1652.

Sekiyama, Y., Chikayama, E., & Kikuchi, J. (2011). Evaluation of a semipolar solvent system as a step toward heteronuclear multidimensional NMR-based metabolomics for (13)C-labeled bacteria, plants, and animals. *Analytical Chemistry*.

Sekiyama, Y., & Kikuchi, J. (2007). Towards dynamic metabolic network measurements by multi-dimensional NMR-based fluxomics. *Phytochemistry*, *68*(16–18), 2320–2329.

Sergeyev, I., & Moyna, G. (2005). Determination of the three-dimensional structure of oligosaccharides in the solid state from experimental ^{13}C NMR data and ab initio chemical shift surfaces. *Carbohydrate Research*, *340*(6), 1165–1174.

Shen, T. Y., Langan, P., French, A. D., Johnson, G. P., & Gnanakaran, S. (2009). Conformational flexibility of soluble cellulose oligomers: Chain length and temperature dependence. *Journal of the American Chemical Society*, *131*(41), 14786–14794.

Somerville, C., Youngs, H., Taylor, C., Davis, S. C., & Long, S. P. (2010). Feedstocks for lignocellulosic biofuels. *Science*, *329*(5993), 790–792.

Suzuki, S., Horii, F., & Kurosu, H. (2009). Theoretical investigations of C-13 chemical shifts in glucose, cellobiose, and native cellulose by quantum chemistry calculations. *Journal of Molecular Structure*, *921*(1–3), 219–226.

Swatloski, R. P., Spear, S. K., Holbrey, J. D., & Rogers, R. D. (2002). Dissolution of cellulose [correction of cellose] with ionic liquids. *Journal of the American Chemical Society*, *124*(18), 4974–4975.

Tian, C., Chikayama, E., Tsuboi, Y., Kuromori, T., Shinozaki, K., Kikuchi, J., et al. (2007). Top-down phenomics of *Arabidopsis thaliana*: metabolic profiling by one- and two-dimensional nuclear magnetic resonance spectroscopy and transcriptome analysis of albino mutants. *Journal of Biological Chemistry*, *282*(25), 18532–18541.

Wickholm, K., Larsson, P. T., & Iversen, T. (1998). Assignment of non-crystalline forms in cellulose I by CP/MAS C-13 NMR spectroscopy. *Carbohydrate Research*, *312*(3), 123–129.

Witter, R., Sternberg, U., Hesse, S., Kondo, T., Koch, F. T., & Ulrich, A. S. (2006). C-13 chemical shift constrained crystal structure refinement of cellulose I-alpha and its verification by NMR anisotropy experiments. *Macromolecules*, *39*(18), 6125–6132.

Zhang, J., Zhang, H., Wu, J., He, J., & Xiang, J. (2010). NMR spectroscopic studies of cellobiose solvation in EmimAc aimed to understand the dissolution mechanism of cellulose in ionic liquids. *Physical Chemistry Chemical Physics*, *12*(8), 1941–1947.

Zhao, H., Jones, C. L., Baker, G. A., Xia, S., Olubajo, O., & Person, V. N. (2009). Regenerating cellulose from ionic liquids for an accelerated enzymatic hydrolysis. *Journal of Biotechnology*, *139*(1), 47–54.

Zhong, R., Demura, T., & Ye, Z. H. (2006). SND1, a NAC domain transcription factor, is a key regulator of secondary wall synthesis in fibers of Arabidopsis. *Plant Cell*, *18*(11), 3158–3170.